A Numerical Elastoplastic Model for Rough Contact

C. Mayeur

P. Sainsot

L. Flamand

Laboratoire de Mécanique des Contacts
(CNRS URA 856),
Institut National des Sciences
Appliquées de Lyon,
69621 Villeurbanne Cedex, France

Pressure distributions due to surface roughness in contact induce high stresses just beneath the surface. These stresses can bring on crack initiation and micro-pitting. A purely elastic contact model to account for these effects is restrictive because stress fields often exceed the yield strength of the material. Plastic flow occurs and modifies the surface shape and material properties (work hardening). This paper presents a numerical model for elastoplastic rough contact. It allows the determination of real pressures and permanent surface displacements (flattening of asperities) as well as residual stress and plastic strains useful in fatigue analysis). The material is assumed to obey the Von-Mises yield criterion with linear kinematic hardening. Real surface profiles obtained from a measurement can be considered. In addition, simplified methods have been used to treat cyclic loading. Thus the ability of a rough surface to reach an elastic shakedown state can be investigated, even for a three-dimensional contact found, for instance, in roller bearings.

Introduction

The rough contact problem has been studied for many years because of its numerous implications in tribology: friction, wear, fatigue, and damage.

The statistical approach, at first investigated by Archard (Archard et al., 1975) and Greenwood and Williamson (1966), yields important results concerning the behavior at the contact scale (contact area, normal approach). However, these models cannot predict local pressure and stress values, which play a major role in material fatigue and damage.

With the increase in computer performance, numerical models have been developed for the study of complex contact problems, (Kalker, 1990). Some of them dealt with rough contact (Webster and Sayles, 1986; Seabra and Berthe, 1987; Bailey and Sayles, 1991; Yonqing and Linqing, 1992). Although these models assumed elastic material behaviour, their results show that this assumption was often improper. On the other hand, the use of a finite element method, which readily treats elastoplastic behavior, leads to costly calculations when both surface roughness and bulk behavior have to be taken into account (Komvopoulos and Choi, 1992).

In order to overcome these difficulties, a numerical method, based on a boundary integral formulation for an elastoplastic half plane, is presented in this paper. Only parts of the half plane where nonlinear response occurs (i.e., contact surface and plastic zone) have to be discretized. The numerical system is thus reduced to a minimum.

Moreover, simplified methods (Zarka et al., 1980; Inglebert et al., 1985; Inglebert and Frelet, 1989) for the analysis of cyclic loading have been used. They allow one to treat the case of a three dimensional rough rolling contact when roughness consists of ridges oriented along the rolling direction. This configuration appears to be representative for ball-raceway contacts of a roller bearing, because of surface manufacturing processes.

Some results are presented in order to illustrate the method.

1 Elastic Contact Model

The main feature of contact consists of the mixed boundary conditions that arise on the contact surface. Furthermore, these boundry conditions are explained with inequalities, and the contact surface is unknown. So, we have to define a potential contact surface Γ_c, that contains the real contact surface. Γ_c is subjected to the boundary conditions:

$$\left.\begin{matrix}\delta \geq 0 \\ p \geq 0\end{matrix}\right\} \text{ on } \Gamma_c \tag{1}$$

p is the local normal contact pressure and δ the local gap between the two bodies. The first condition is a non penetration condition, and the second implies that normal tractions are only compressive. δ can be written as:

$$\delta = u + h \tag{2}$$

where u is the normal displacement difference and h is the initial distance between the two bodies.

Each body has to satisfy stress equilibrium (bulk equation) and is submitted to additional classical boundary conditions, i.e., displacements and/or forces prescribed on some parts of its surface. When the contact area is small compared to the dimensions of the body, and when surface slopes are small,

Contributed by the Tribology Division of The American Society of Mechanical Engineers and presented at the ASME/STLE Tribology Conference, Maui, Hawaii, October 16-19, 1994. Manuscript received by the Tribology Division March 1, 1994; revised manuscript received July 25, 1994. Paper No. 94-Trib-59. Associate Technical Editor: K. Komvapoulos.

the solids in contact can be considered as two half spaces. The Boussinesq relations between load and displacement at the surface can then be used (Johnson, 1985). In addition, this assumption enables the substitution of the classical boundary conditions (displacements or forces prescribed) by a load or rigid body movement condition. The use of the Boussinesq load-displacement relation leads to:

$$u(x) = \int_{\Gamma_c} U(x, \xi) p(\xi) d\Gamma(\xi) \tag{3}$$

where x and ξ are two points on the surface, and $U(x, \xi)$ is the displacement at point x due to a unit load at point ξ.

This relation verifies stress equilibrium, elastic behavior and small strains assumption. As Γ_c is unknown, the procedure is iterative. This problem can be solved for either 2-D or 3-D contacts (Seabra and Berthe, 1987, Yonqing and Linqing, 1992), and measured surface profiles can be considered (Webster and Sayles, 1986, Bailey and Sayles, 1991).

Based on the half space assumption, many models have been proposed to solve different types of contact problems: smooth or rough surface, only normal or normal and tangential tractions, etc. In this paper we only consider normal contact of two bodies (tangential tractions are supposed to be nil). The model proposed by Seabra and Berthe (1987), which allows short CPU times, is used.

2 Elastoplastic Behavior

2.1 Constitutive Law. Elastoplastic material behavior is characterized by the appearance of strains which are instantaneous, irrecoverable, and are submitted to a threshold condition. The first characteristic means that plasticity is time independent, but the two others imply that it is a path dependent (dissipative) phenomenon.

Many different behaviors have been observed above the elastic limit, concerning materials and loading conditions. Thus many constitutive laws have been proposed to describe plasticity. Here we consider a material that obeys to the Von-Mises yield function and presents a linear kinematic hardening. These assumptions are quite suitable to represent metal behavior (Ham et al., 1989, Hahn and Rubin, 1991), especially for cyclic loading, and are easy to take into account in a numerical procedure.

The yield condition is defined by:

$$f(\sigma_{ij}, \epsilon^p_{ij}) = \sqrt{\frac{3}{2}(s_{ij} - C\epsilon^p_{ij})(s_{ij} - C\epsilon^p_{ij})} \le \sigma_y,$$

$$\text{with } s_{ij} = \sigma_{ij} - \frac{1}{3}\sigma_{kk}\delta_{ij} \tag{4}$$

s_{ij} are the deviatoric stress tensor components, ϵ^p_{ij} the plastic strain tensor components, C the hardening modulus, σ_y the elastic limit in traction and δ_{ij} the Kronecker symbol. In a nine dimensional space (the deviatoric stress space), the elastic domain is represented by a sphere of radius $\sqrt{2/3}\ \sigma_y$ which has a translation proportional to plastic strain rates.

Plastic flow is governed by:

$$\dot{\epsilon}^p_{ij} = \frac{3}{2C\sigma_y^2}[(s_{ij} - C\epsilon^p_{ij})\dot{s}_{ij}](s_{ij} - C\epsilon^p_{ij})$$

$$\text{if } f(\sigma_{ij}, \epsilon^p_{ij}) = \sigma_y \text{ and } \frac{\partial f}{\partial s_{ij}}\dot{s}_{ij} > 0 \tag{5}$$

where the dot denotes the rate of the variables.

2.2 Simplied Methods for the Analysis of Structures Under Cyclic Loading. In the case of a cyclic loading, the structure can respond as:

(*1*) *purely elastic*: no plastic strain occurs, the structures stays always in the elastic domain;

(*2*) *elastic shakedown*: plasticity occurs at the early cycles, but both residual stresses and work hardening generated by plastic strains result in a purely elastic stabilized state;

(*3*) *plastic shakedown* (*or cyclic plasticity*): plasticity occurs at each cycle, and residual stresses and plastic strains reach a cyclic stabilized state;

(*4*) *incremental collapse* (*or ratchetting*): plasticity occurs at each cycle, and no stabilized state can be reached.

The two first possible regimes protect the structure, which will be able to support many load cycles. The two others, where dissipative processes occur at each cycle, result in an early failure. Knowledge of the stabilized regime associated to a structure and loading conditions is thus crucial for fatigue considerations.

As plasticity is path dependent, the associated constitutive laws are incremental and numerical procedures are iterative. In the case of cyclic loading, determination of the stabilized state, which can be reached after many cycles, implies high computational costs for such a process. In order to reduce

Nomenclature

h = initial local distance between two bodies
k = shear yield strength
p = local pressure on the surface
s = deviatoric stress tensor
s^e = elastic deviatoric stress tensor
s^r = residual deviatoric stress tensor
u = displacement vector
u^e = elastic displacement vector
u^r = residual displacement vector
C = hardening modulus
C_{klij} = influence functions of plastic strains upon stresses
D_{jki} = influence functions of plastic strains upon displacements
E = Young modulus
$[M]$ = elasticity matrix
N_c = number of points on Γ_c
N_i = number of points of Γ_c inside the real contact area
N_e = number of point of Γ_c outside the real contact area
N_p = number of points in Ω_p
S_{kij} = influence functions of pressure upon stresses
U_{ji} = influence functions of pressure upon displacements
Y = transformed parameter (tensor)
δ = local distance between two bodies
δ_{ij} = Kronecker symbol
ϵ^p = plastic strain tensor
ϵ = strain tensor
ϵ^e = elastic strain tensor
ϵ^r = residual strain tensor
ν = Poisson coefficient
σ = stress tensor
σ^e = elastic stress tensor
σ^r = residual stress tensor
σ_y = traction yield strength
Γ_c = potential contact surface
Ω_p = plastic zone

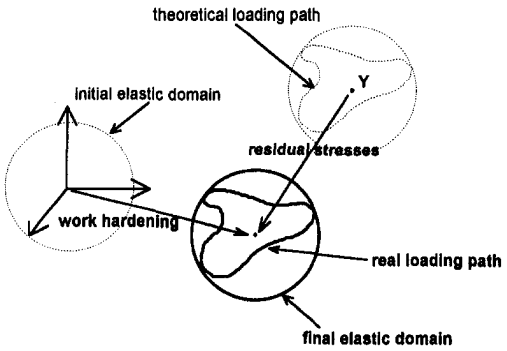

Fig. 1 Schematic of elastic shakedown in deviatoric stress space; definition of point Y

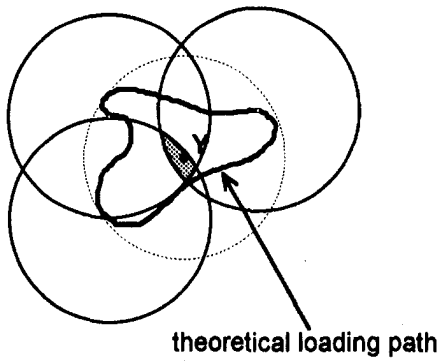

Fig. 2 Potential zone for point Y

computer time, Zarka et al. (1980) and Ingelbert et al. (1985, 1989) have proposed simplified methods to determine the stabilized state under cyclic loading for elastoviscoplastic materials. These methods allow short CPU times. Only the theoretical elastic stresses (when no plasticity occurs) are needed. The case of elastic shakedown for an elastoplastic material with linear kinematic hardening will be presented here.

Initially for each material point, all the theoretical (elastic) states of stress $\sigma^e(t)$ applied during a cyclic loading form in deviatoric stress space a closed loop, called the theoretical loading path. This loop is partially or totally out of the initial elastic domain, so plasticity occurs.

When elastic shakedown is achieved, the elastic domain has been translated, due to work hardening; furthermore a set of constant residual stresses has appeared, so the real loading path (elastic stresses and residual stresses) can be deduced from the theoretical loading path with another translation. These two modifications are such that the final loading path remains totally within the final elastic domain (Fig. 1).

If the theoretical loading path lies totally in the initial elastic domain, purely elastic behavior occurs: on the other hand, if no relative position for elastic domain and loading path can be found to ensure elastic behavior (the loading path is too important for the elastic domain), plastic shakedown or incremental collapse takes place.

When the elastic shakedown is reached, the Von-Mises yield function implies for every time t:

$$\sqrt{\frac{3}{2}(s_{ij}(t)-C\epsilon^p_{ij})(s_{ij}(t)-C\epsilon^p_{ij})} \le \sigma_y \tag{6}$$

The total stress tensor can be expressed as follows:

$$\sigma = \sigma^e + \sigma^r \tag{7}$$

σ^e is the theoretical elastic stress tensor, which corresponds to the external loading, and σ^r is the residual stress tensor, which is related to the induced plastic strains.

Then the deviatoric stress tensor reads:

$$s = s^e + s^r \tag{8}$$

We now introduce a new tensor Y defined as:

$$Y = C\epsilon^p - s^r \tag{9}$$

The parameter Y contains all the terms of the yield function related to plastic stains, and is time-independent when elastic shakedown is reached. The Von-Mises criterion expressed in terms of Y becomes:

$$\sqrt{\frac{3}{2}(s^e_{ij}(t)-Y)(s^e_{ij}(t)-Y_{ij})} \le \sigma_y \tag{10}$$

Thus, in deviatoric stress space, Y is the center of a sphere which has the same radius as the elastic domain, and which contains all the theoretical states of stress (Fig. 1). On the other hand, if we consider spheres of same radius than the elastic domain but centered at each loading point, point Y lies inside each sphere (Fig. 2). The intersection of all the above spheres is the potential domain for point Y.

When loading path is large compared to the size of elastic domain, the potential domain for point Y is small and then a good accuracy can be obtained. In the general case, Inglebert and Frelat (1989) have found that a good approximation could be obtained by the projection of the initial value of Y on the intersection domain. In the case of a linear loading, i.e., the loading path is a straight line, only the two extreme loading points have to be taken into account, and the projection of the initial state is quite easy.

Once the Y are known for each plastic point of the structure, one has to determine the plastic strains and residual stresses. Inglebert and Frelat (1989) use a particularly attractive method which only needs an elastic calculation using finite element methods, plastic behavior being substituted by fictitious changes in elastic properties. However, this method is not used here because of the unsuitable use of the finite element method to describe the rough contact problem.

3 Boundary Integral Formulation

In this section, only the plane strain elastoplastic contact will be discussed. The simplified methods presented above do not need to model the elastoplastic (incremental) loading. For a tridimensional rolling contact, if roughness is taken as constant along the rolling direction, the residual state stays constant along this direction. Thus only a two-dimensional problem has to be solved in this case. Furthermore, the loading path is nearly linear so the projection of parameters Y is quite easy.

When the contact area is small compared to the dimensions of bodies, the extent of the plastic zone is small. As discussed before, finite element methods, which need a discretization of the entire bodies to represent bulk behavior, lead to costly calculations for modelling a rough contact, even with the simplified methods presented above where a step-by-step analysis is not necessary. Keeping the half plane assumption, often used in contact mechanics, a boundary integral formulation is used, which allows to discretize only the zone where plasticity occurs (in addition to contact surface).

When a half plane is subjected to a load distribution at its surface Γ, together with an inelastic strain distribution in its volume Ω, displacements at each point ξ can be expressed as follows:

$$u_i(\xi) = \int_\Gamma u^*_{ij}(\xi, x)p_j(x)d\Gamma(x) + \int_\Omega [\sigma^*_{jki}(\xi, x) - \nu\sigma^*_{lli}(\xi, x)]d\Omega(x) \tag{11}$$

where $u^*_{ij}(\xi, x)$ and $\sigma^*_{jki}(\xi, x)$ correspond, respectively, to components (j) and (jk) of displacement and stress at point x due to a unit force applied in direction (i) at point ξ in a half plane.

This expression has been proposed by Telles and Brebbia (1981), and is derived from the application of the Somiglia identity for elastic material with initial strains, using the fundamental solution of a half plane domain with a free boundary; using this formulation, a distinct class of boundary element methods has been successfully used in soil mechanics problems (Telles and Brebbia, 1981, Brebbia et al., 1984).

The application of a boundary integral formulation implicitly accounts for the elastic (linear) part of the material behavior in bulk. The use of the half plane fundamental solution implicitly accounts for the geometry Thus, only the discretization of the loading surface Γ_c and the plastic zone Ω_p is necessary.

As discussed before, the elastoplastic stress tensor σ is divided into an elastic part σ^e and a residual part σ^r:

$$\sigma = \sigma^e + \sigma^r$$

The corresponding strains are:

$$\epsilon = \epsilon^e + \epsilon^r \tag{12}$$

They are related to the stresses by:

$$\epsilon = [M]\sigma \tag{13}$$

$$\epsilon^e = [M]\sigma^e \tag{14}$$

$$\epsilon^r = [M]\sigma^r + \epsilon^p \tag{15}$$

where $[M]$ is the elasticity matrix.

Following the same procedure, displacements can be expressed as:

$$u = u^e + u^r \tag{16}$$

where u^e and u^r are defined by:

$$u_i^e(\xi) = \int_\Gamma u_{ij}^*(\xi, x) p_j(x) d\Gamma(x) \tag{17}$$

$$u_i^r(\xi) = \int_\Omega [\sigma_{jki}^*(\xi, x) - \nu\sigma_{lli}^*(\xi, x)]\epsilon_{jk}^p(x)\, d\Omega(x) \tag{18}$$

Each of these two parts has a physical meaning: u^e corresponds to the solution for a purely elastic material, and u^r corresponds to the stabilized state when the half plane is unloaded, if no plasticity occurs during unloading (as is the case for elastic shakedown).

From a mathematical point of view, u^e is the solution of the associated homogeneous problem of elasticity with initial strains which satisfy the boundary conditions, and u^r is a specific solution of the total problem which does not modify the boundary conditions.

4 Resolution/Numerical Procedure

4.1 Discretization. Following Seabra and Berthe (1987), the potential contact surface Γ_c is discretized into N_c elements of the same size where the pressure is assumed to be constant. N_i and N_e are the number of elements of Γ_c inside and outside the real contact area ($N_i + N_e = N_c$).

Furthermore, the plastified volume is discretized into N_p rectangular cells where plastic strains are assumed to be constant. Equation (11) can be rewritten as:

$$u_i(\xi) = \sum_{n=1}^{N_i} \left\{ \int_{\Gamma_n} u_{ij}^*\, d\Gamma \right\} p_j(n) + \sum_{m=1}^{N_p} \left\{ \int_{\Omega_m} [\sigma_{jki}^* - \nu\sigma_{lli}^*] d\Omega \right\} \epsilon_{jk}^p(m) \tag{19}$$

where Γ_n and Ω_p are the local domains associated to elements n and m.

Contrary to the classical boundary element method, integrals over each element are calculated analytically, as it is allowed by the simple interpolation (constant). Therefore, Eq. (19) results in:

$$u_i(\xi) = \sum_{n=1}^{N_i} U_{ji}(n, \xi) p_j(n) + \sum_{m=1}^{N_p} D_{jki}(m, \xi)\epsilon_{jk}^p(m) \tag{20}$$

Uji and Djki are analytical functions for the point ξ. They can be derived and combined to give the stress components in the form:

$$\sigma_{ij}(\xi) = \sum_{n=1}^{N_i} S_{kij}(n, \xi) p_k(n) + \sum_{m=1}^{N_p} C_{klij}(m, \xi)\epsilon_{jk}^p(m) \tag{21}$$

Expressions of U_{ij} and S_{kij} correspond to displacements and stresses due to a rectangular distribution of pressure on the half plane surface and can be found in Johnson (1985). Expressions of D_{jki} and C_{klij} are the displacements and stresses due to a uniform distribution of plastic strains in a rectangular cell and are given in the Appendix. The use of a constant discretization step leads to a reduced number of stored coefficients.

Relations (1), (2), and (9) are then discretized, and the two following systems of equations are given:

Elastic System

$$u_i^e(n) = \sum_{m=1}^{N_i} U_{ji}(m, n) p_j(m) \quad n = 1, N_c \tag{22}$$

$$u^e(n) + u^r(n) + h(n) = 0 \quad n = 1, N_j \tag{23}$$

$$p(n) = 0 \quad n = 1, N_e \tag{24}$$

$$u^e(n) + u^r(n) + h(n) > 0 \quad n = 1, N_e \tag{25}$$

$$p(n) > 0 \quad n = 1, N_i \tag{26}$$

When the pressure distribution on Γ_c is known, elastic stresses in bulk can be obtained using:

$$\sigma_{ij}^e(\xi) = \sum_{n=1}^{N_i} S_{kij}(n, \xi) p_k(n) \tag{27}$$

Residual System

$$\sigma_{ij}^r(n) = \sum_{m=1}^{N_p} C_{klij}(m, n)\epsilon_{kl}^p(m) \quad n = 1, N_p \tag{28}$$

$$\epsilon^p(n) = \frac{1}{C}\,(Y(n + s^r(n))) \quad n = 1, N_p \tag{29}$$

Once the ϵ^p values are known, displacements on the surface can be obtained using:

$$u_i^r(n) = \sum_{m=1}^{N_p} D_{kli}(m, n)\epsilon_{kl}^p(m) \quad n = 1, N_c \tag{30}$$

Only normal displacements will be computed. Tangential displacements are neglected.

4.2 Resolution

Elastic Problem. For a given distribution of u^r, the elastic problem corresponds to an elastic contact problem with an apparent distance $u^r + h$ instead of h. It has been solved using Seabra and Berthe's method. Then elastic stresses are computed using Eq. (27).

Residual Problem. For a given stress field σ^e, parameters Y are obtained using projection techniques proposed by Ingelbert and Frelat (1989). The loading path is assumed to be linear between zero and the maximum value of the Von-Mises equivalent stress. Equations (28) and (29) can be combined to form a linear system. Nevertheless, we solve this problem using an iterative process. Initially, residual stresses are supposed to be zero and plastic strains are: $\epsilon^p = 1/C\ Y$. Then Eqs. (28) and (29) are used successively to determine new stresses and new plastic strains until convergence. During this process, under relaxation of ϵ^p is used in order to reduce the number of iterations. No convergence difficulties have been noticed with values of hardening modulus over 30000 MPa.

Below this value, material behavior approaches perfect plasticity (no work-hardening) and numerical problems arise.

Once the solution is obtained for ϵ^p and σ^r, the displacements u^r are calculated using (30).

4.3 Coupling of the Two Parts. The two parts u^e and u^r are dependent. Each is the solution of a problem where the other is assumed to be known. Thus another iterative process is used. Initially, we suppose that no plasticity occurs and elastic contact is solved with the conditions:

$$\begin{cases} h + u^e \geq 0 \\ \sigma^e n \geq 0 \end{cases}$$

The resulting stresses σ^e are used to determine the corresponding ϵ^p, σ^r, and u^r. Then u^r is used to solve another contact problem and this procedure is repeated until convergence. Under relaxation of u^r is used to improve convergence.

Note that Eq. (11) can be used in an incremental form with a real plastic flow constitutive law for a step by step analysis. Keeping the influence coefficients in memory, a performing iterative process can be obtained. However, this can only be done easily in plane strain or plane stress cases, but it would need a large memory capacity for a real tridimensional problem.

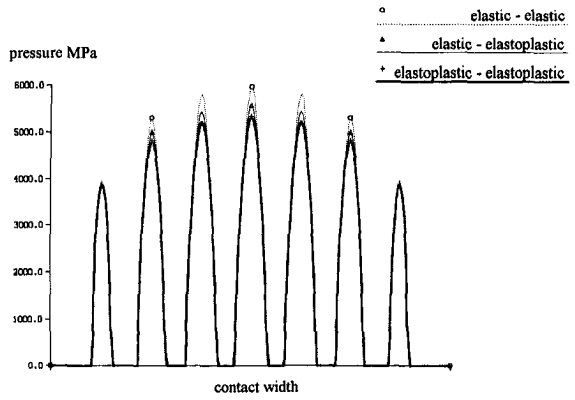

Fig. 3 Pressure distributions for various combinations of body behaviors; $k = 1000$ MPa, $C = 88000$ MPa

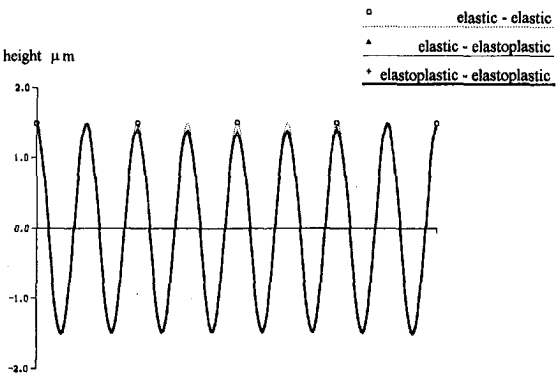

Fig. 4 Surface profiles after unloading for various combinations of body behaviors; $k = 1000$ MPa, $C = 88000$ MPa.

5 Results and Discussion

The aim of this section is to illustrate the ability of the model to deal with elastoplastic rough contact. A more detailed study will be done later.

For convenience, all the results are presented for bidimensional contact cases. They correspond to the plane strain indentation of a rough body by a smooth one, both having the same elastic properties:

$$E = 210000 \text{ MPa}$$

$$\nu = 0.3$$

For the two first examples, roughness is modelled by a sinusoidal surface profile, of wavelength 0.15 mm and amplitude 1.5 μm. 201 points have been used along surface axis (1.2 mm) and 11 through the depth (0.11 mm). The contact half width is 0.5 mm and the corresponding Hertz pressure for two smooth surfaces is 2500 MPa.

Figures 3 and 4 show the pressure distributions and surface profiles (after unloading) for three cases:

(1) the two bodies are elastic (E-E);

(2) the body with the wavy surface is elastoplastic (E-EP);

(3) the two bodies are elastoplastic with similar properties (EP-EP).

The following elastoplastic parameters have been used:

$$k = 1000 \text{ MPa}$$

$$C = 88000 \text{ MPa}$$

k is the elastic limit in shear ($k = \sigma_y/\sqrt{3}$).

Table 1 gives the relative deviation (in percent) for different contact parameters when the resolution of the discretization differs.

As no derivative or integral is performed numerically, deviations are small as long as the discretization is fine enough to approximate surface profile and elastic stress field in bulk.

Figures 5 and 6 show the same results with different elastoplastic parameters:

$$k = 800 \text{ MPa}$$

$$C = 53300 \text{ MPa}$$

The surface profiles show that as asperity summits are crushed, valleys move up, but in a slighter way. The hypothesis

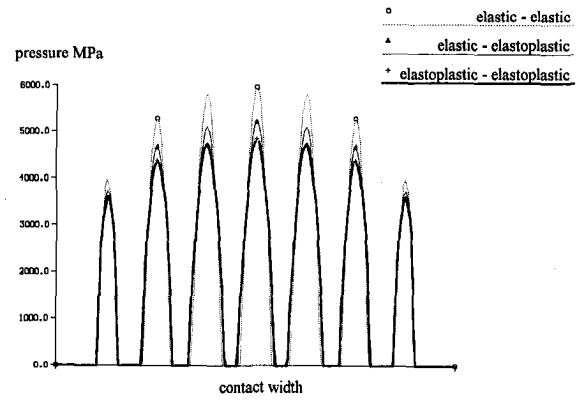

Fig. 5 Pressure distributions for various combinations of body behaviors; $k = 800$ MPa, $C = 53300$ MPa.

Table 1 Relative deviation (in percent) of contact parameters as a function of the discretization size

Number of points (width*depth)	Maximum pressure for E-E contact	Maximum pressure for E-EP contact	Maximum pressure for EP-EP contact	Maximum surface residual displacement	Maximum equivalent plastic strain	Maximum Von-Mises residual stress
101 * 11	0,44	0,44	0,62	1,51	0,16	1,61
301 * 11	0,07	0,14	0,16	1,50	0,32	2,87
201 * 6	0,00	0,09	2,41	6,53	2,70	14,05
201 * 21	0,00	0,28	0,62	0,50	1,27	0,22

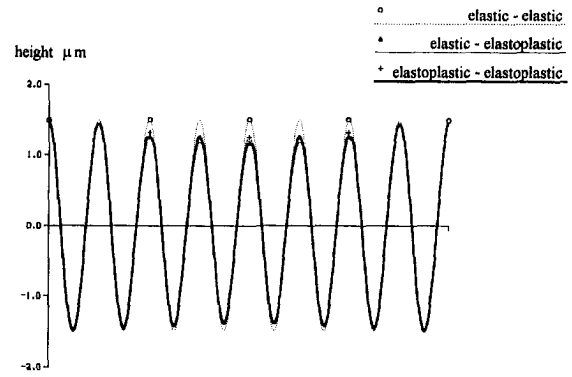

Fig. 6 Surface profiles after unloading for various combinations of body behaviors; $k = 800$ MPa, $C = 53300$ MPa

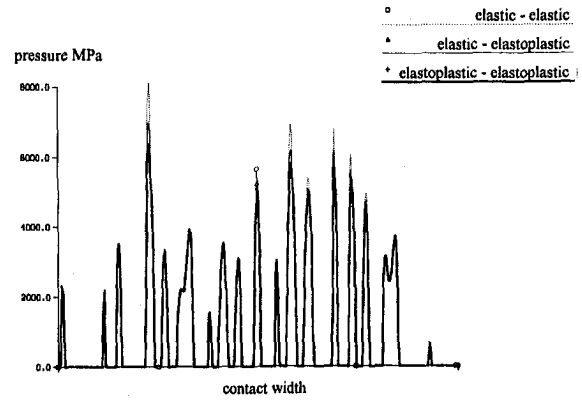

Fig. 7 Pressure distributions for various combinations of body behaviors; $k = 1000$ MPa, $C = 88000$ MPa

of asperity volume conservation, suggested by incompressibility of plastic strains and met sometimes in statistical rough elastoplastic contact models (Chang et al., 1987), seems somewhat excessive. In reality, plasticity occurs in a zone greater than asperity volume (subsurface plastic flow), and both plastic and elastic strains are of the same order.

For a current elastoplastic structure, elastic shakedown is reached through two mechanisms:

—residual stresses (structural effect), which reduce the applied stresses;

—work-hardening (material effect), which modifies the elastic domain.

As pointed out by Johnson (1987) for a smooth contact, a third mechanism to reach shakedown appears in contact problems. It is the issue of the mixed boundary condition on the contact surface (conformity effect): plastic strains, which modify the asperity shape, leads to reduced pressures and stresses.

More recently, Johnson and Shercliff (1992), and Kapoor and Johnson (1993) have studied the steady state topography of rough surfaces, assuming that deformed asperities are such that pressure do not exceed the shakedown limit.

However, our results show that with the parameters used in this paper (corresponding to bearing steel properties), and when considering only normal contact and normal displacements, the major contribution to shakedown comes from the material behavior. Structural and conformity effects are limited because of the reduced plastic strains due to work-hardening.

Figure 7 shows the pressure field obtained from a measured surface profile. The same material properties as in Figs. 3 and 4 are used. 351 points are used to describe the profile (0.35 mm) and 20 points are taken along depth axis (20 μm). The contact half-width is 0.15 mm, and the equivalent Hertz pressure is 1500 MPa.

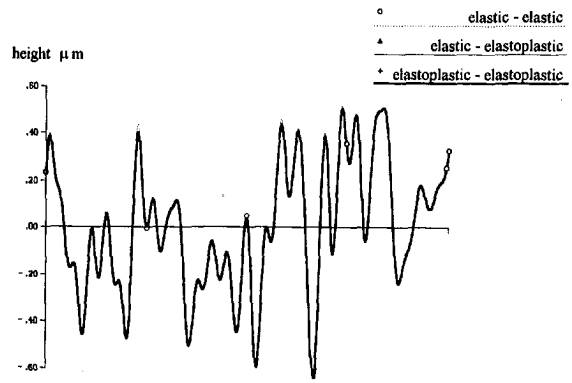

Fig. 8 Surface profiles after unloading for various combinations of body behaviors; $k = 1000$ MPa, $C = 88000$ MPa

The reduction of the pressure peaks is more important in this realistic case because of the initial sharpness of the asperities (Fig. 8). But the summits of a few asperities are only lightly flattened, and the increase in contact conformity due to plastic strains is small.

In this case, the decreases in pressure are sufficient to make the surface reach an elastic shakedown state for the elastoplastic/elastoplastic contact, but not for the elastic/elastoplastic contact.

Surface geometrical changes seem to be too light to represent the running-in process, and wear must occur first in this case.

However, not that the depths concerned with plastic strains are small (less than 50 μm), so that the material properties and the initial state (residual stresses and work hardening due to manufacturing process) of this thin layer can be very different from bulk behavior. A better knowledge of this real behavior is necessary.

6 Conclusion

A full numerical model of plane strain elastoplastic rough contact problem is presented. Based on a semi-analytical approach (half plane assumption and boundary integral formulation), it allows one to discretize only the contact surface and the plasticity deformed zone.

Furthermore, simplified methods for the analysis of elastoplastic structures are used in order to study the ability of a rough surface to reach an elastic shakedown state. These methods permit the investigation of the case of tridimensional rolling contact when roughness is composed of ridges along the rolling direction, as it is the case for ball-raceway contacts in a roller bearing.

The resulting values of residual stresses and plastic strains beneath the surface can be useful for fatigue contact analysis.

In an incremental form, the boundary integral formulation can be combined with real plastic flow constitutive laws in order to model a real loading path in plane strain.

In this study, the whole problem is divided into an elastic part, which corresponds to a classical elastic contact problem, and a residual part, which accounts for plastic flow in bulk. The originality of this work lies in the treatment of the residual problem. The elastic part is considered as a normal, dry, frictionless contact.

Therefore, the residual part can be coupled with a more complex elastic problem as, for example, elastohydrodynamic or dry frictional contacts.

Acknowledgments

This study has been supported by SEP (Societé Européenne de Propulsion), CNRS (Centre National de la Recherche Scientifique) and CNES (Centre National d'Etudes Spatiales) as part of GdR (Groupement de Recherche) 0916.

References

Archard, J. F., Hunt, R. T., and Onions, R. A., 1975, "Stylus Profilometry and the Analysis of the Contact of Rough Surfaces," *The Mechanics of the Contact Between Deformable Bodies*, Delft University Press, pp. 282–303.

Bailey, D. M., and Sayles, R. S., 1991, "Effect of Roughness and Sliding Friction on Contact Stresses," ASME JOURNAL OF TRIBOLOGY, Vol. 113, pp. 729–738.

Brebbia, C. A., and Telles, J. F. C., and Wrobel, L. C., 1984, *Boundary Element Techniques*, Springer-Verlag, Berlin, 466 pp.

Chang, W. R., Etsion, I., and Bogy, D. B., 1987, "An Elastic-Plastic Model for the Contact of Rough Surfaces," ASME JOURNAL OF TRIBOLOGY, Vol. 119, pp. 257–263.

Greenwood, J. A., and Williamson, J. B. P., 1966, "Contact of Nominally Flat Surfaces," *Proc. Roy. Soc.*, London, Vol. 295, pp. 300–319.

Hahn, G. T., and Rubin, C. A., 1991, "Elastoplastic Analysis of Repeated Rolling and Sliding Contact," *Advances in Engineering Tribology*, STLE SP-31, pp. 55–70.

Ham, G. L., Hahn, G. T., Rubin, C. A., and Bhargava, V., 1989, "Finite Element Analysis of the Influence of Kinematic Hardening in Two-Dimensional, Repeated, Rolling-Sliding Contact," *Trans. STLE*, Vol. 32, pp. 311–316.

Inglebert, G., Frelat, J., and Proix, J. M., 1985, "Structures Under Cyclic Loading," *Arch. Mech.*, Vol. 37, pp. 365—382.

Inglebert, G., and Frelat, J., 1989, "Quick Analysis of Inelastic Structures Using a Simplified Method," *Nuclear Engineering and Design*, Vol. 116, pp. 281–291.

Johnson, K. L., 1985, *Contact Mechanics*, Cambridge University Press, Cambridge, 417 p.

Johnson, K. L., 1987, "Plastic Flow, Residual Stress and Shakedown in Rolling Contact," *Contact Mechanics and Wear of Rail/Wheel Systems II*, University of Waterloo Press, pp. 83–98.

Johnson, K. L., and Shercliff, H. R., 1992, "Shakedown of 2-Dimensional Asperities in Sliding Contact," *International Journal of Mechanical Science*, Vol. 34, pp. 375–394.

Kalker, J. J., 1990, *Three-Dimensional Elastic Bodies in Rolling Contact*, Kluwer Academic Publishers, Dordrecht, 314 pp.

Kapoor, A., and Johnson, K. L., 1993, "Steady State Topography of Surfaces in Repeated Boundary Lubricated Sliding," *Proc. 19th Leeds-Lyon Symposium on Tribology*, pp. 81–90.

Komvopoulos, K., and Choi, D. H., 1992, "Elastic Finite Element Analysis of Multi-Asperity Contacts," ASME JOURNAL OF TRIBOLOGY, Vol. 114, pp. 823–831.

Seabra, J., and Berthe, D., 1987, "Influence of Surface Waviness and Roughness on the Normal Pressure Distribution in the Hertzian Contact," ASME JOURNAL OF TRIBOLOGY, Vol. 109, pp. 462–470.

Telles, J. F. C., and Brebbia, C. A., 1981, "New Developments in Elastoplastic Analysis," *Boundary Element Methods*, Springer-Verlag, pp. 350–370.

Webster, M. N., and Sayles, R. S., 1986, "A Numerical Model for the Elastic Frictonless Contact of Real Rough Surfaces," ASME JOURNAL OF TRIBOLOGY, Vol. 108, pp. 314–320.

Yonqing, J., and Linqing, Z., 1992, "A Full Numerical Solution for the Elastic Contact of Three Dimensional Real Rough Surfaces," *Wear*, Vol. 157, pp. 151–161.

Zarka, J., Engel, J. J., and Ingelbert, G., 1980, "On a Simplified Inelastic Analysis of Structures," *Nuclear Engineering and Design*, Vol. 57, pp. 333–368.

APPENDIX

Displacements and Stresses Due to a Constant Distribution of Plastic Strains in a Rectangular Domain of a Half Plane

We consider the displacement and stress fields due to a rectangular constant plastic strain distribution in a half plane (Fig. A.1). **X** (X_1, X_2) is the middle of the rectangle and $2\Delta_1$, $2\Delta_2$ are the side lengths.

$D_{jki}(\xi, \mathbf{X})$ is the component along i of displacement at point $\xi(\xi_1, \xi_2)$ due to a constant distribution of component ϵ_{jk} of plastic strains, and $C_{klij}(\xi, \mathbf{X})$ is the component σ_{ij} of stress at point ξ due to a constant distribution of component ϵ_{kl} of plastic strains.

Displacements:

Displacement functions D_{jki} involve the values of a function $\overline{D}_{jki}$ at each corner of the rectangle as follows:

$$D_{jki}(\xi_1, \xi_2, X_1, X_2) = \overline{D}_{jki}(\xi_1, \xi_2, X_1+\Delta_1, X_2+\Delta_2) - \overline{D}_{jki}(\xi_1, \xi_2, X_1+\Delta_1, X_2-\Delta_2) + \overline{D}_{jki}(\xi_1, \xi_2, X_1-\Delta_1, X_2-\Delta_2) - \overline{D}_{jki}(\xi_1, \xi_2, X_1-\Delta_1, X_2+\Delta_2)$$

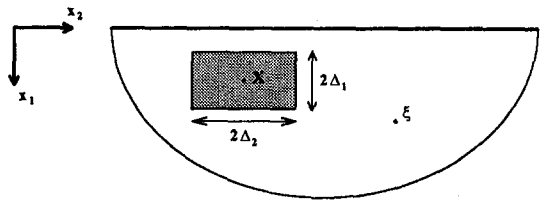

Fig. A1 Constant plastic strain distribution in a rectangular domain of a half plane

Analytical expressions for functions $\overline{D}_{jki}$ are given below.

$$\overline{D}_{111} = K_s\left\{-(3-4\nu)r_2\ln r + 2(1-2\nu)r_1(\theta_1+\alpha_1) - [(1-2\nu)^2 + 4(1-\nu)^2]r_2 \ln R + 2(1-2\nu)^2 R_1(\theta_2+\alpha_2) + \frac{2\xi_1 x_1 r_2}{R^2}\right\}$$

$$\overline{D}_{112} = K_s\left\{r_1\ln r + [[-(1-2\nu)^2 + 4\nu(1-\nu)]R_1 - 2(3-4\nu)\xi_1] \times \ln R - 4(1-\nu)(1-2\nu)r_2(\theta_2+\alpha_2) + \frac{2\xi_1 x_1 R_1}{R^2}\right\}$$

$$\overline{D}_{121} = K_s\left\{-(1-2\nu)r_1\ln r - 2(1-\nu)r_2\theta_1 + (1-2\nu)r_1\ln R - 2(1-\nu)r_2\theta_2 + 2(1-\nu)(1-2\nu)r_2\alpha_2 - \frac{2\xi_1 x_1 R_1}{R^2}\right\}$$

$$\overline{D}_{122} = K_s\left\{(1-2\nu)r_2\ln r + 2(1-\nu)r_1(\theta_1+\alpha_1) + (1-2\nu)r_2\ln R + 2(1-\nu)r_1\theta_2 + 2(1-\nu)R_1\alpha_2 + \frac{2\xi_1 x_1 r_2}{R^2}\right\}$$

$$\overline{D}_{221} = K_s\left\{r_2\ln r + [-(1-2\nu)^2 + 4\nu(1-\nu)]r_2\ln R - 4(1-\nu) \times [-(1-\nu)R_1 + \xi_1]\theta_2 + 4(1-\nu)(1-2\nu)R_1\alpha_2 - \frac{2\xi_1 x_1 r_2}{R^2}\right\}$$

$$\overline{D}_{222} = K_s\left\{-(3-4\nu)r_1\ln r - 2(1-2\nu)r_2\theta_1 + [-[(1-2\nu)^2 + 4(1-\nu)^2]R_1 + 2\xi_1]\ln R - 2(1-2\nu)^2 r_2\theta_2 \geq \frac{2\xi x_1 R_1}{R^2}\right\}$$

with:

$$K_s = \frac{1}{4\pi(1-\nu)}$$

$$r_i = x_i - \xi_i \qquad R_1 = x_1 + \xi_1$$

$$r = \sqrt{r_1^2 + r_2^2} \qquad R = \sqrt{R_1^2 + r_2^2}$$

$$\theta_1 = \arctan\left(\frac{r_1}{r_2}\right) \qquad \theta_2 = \arctan\left(\frac{R_1}{r_2}\right)$$

$$\alpha_1 = \begin{cases} 0 \text{ if } \dfrac{r_1}{r_2} > 0 \\ \pi \text{ if } \dfrac{r_1}{r_2} < 0 \end{cases} \qquad \alpha_2 = \begin{cases} 0 \text{ if } \dfrac{R_1}{r_2} \geq 0 \\ \pi \text{ if } \dfrac{R_1}{r_2} < 0 \end{cases}$$

Stresses:

As for displacement functions, stress functions C_{klij} involve the values of a function $\overline{C}_{jkij}$ at each corner of the rectangle, in addition with a constant term f_{klij} as follows:

$$C_{klij}(\xi_1, \xi_2, X_1, X_2) = \overline{C}_{klij}(\xi_1, \xi_2, X_1+\Delta_1, X_2+\Delta_2) - \overline{C}_{klij}(\xi_1, \xi_2, X_1+\Delta_1, X_2-\Delta_2) + C_{klij}(\xi_1, \xi_2, X_1-\Delta_1, X_2-\Delta_2) - C_{klij}(\xi_1, \xi_2, X_1-\Delta_1, X_2+\Delta_2) + f_{klij}$$

If the point ξ is out of the rectangle, all the terms f_{klij} are nil. If ξ is inside the rectangle, all the terms f_{klij} are nil except:

$$f_{1122} = \frac{\nu E}{1-\nu^2} \text{ and } f_{2222} = -\frac{E}{1+\nu}.$$

Analytical expressions for functions $\overline{C}_{klij}$ are given below.

$$\overline{C}_{1111} = K_e \left\{ \frac{r_1 r_2}{r^2} - 2(1-\nu)(\theta_1+\alpha_1) + \frac{[-(3-4\nu)\xi_1 - x_1]}{R^2} - \frac{4\xi_1 x_1 R_1 r_2}{R^4} + 2(1-\nu)(\theta_2+\alpha_2) \right\}$$

$$\overline{C}_{1112} = K_e \left\{ -\frac{r_1^2}{r^2} + (1-2\nu)\ln r + \frac{x_1^2 - (3-4\nu)\xi_1^2 - 4(1-\nu)\xi_1 x_1}{R^2} + \frac{4\xi_1 x_1 r_2^2}{R^4} - (1-2\nu)\ln R \right\}$$

$$\overline{C}_{1122} = K_e \left\{ -\frac{r_1 r_2}{r^2} - 2\nu(\theta_1+\alpha_1) + \frac{[-3x_1 + (3-4\nu)\xi_1]r_2}{R^2} + \frac{4\xi_1 x_1 R_1 r_2}{R^4} + 2(2-3\nu)(\theta_2+\alpha_2) \right\}$$

$$\overline{C}_{1211} = K_e \left\{ -\frac{r_1^2}{r^2} + \ln r + \frac{x_1^2 + \xi_1^2 + 4\xi_1 x_1}{R^2} - \frac{4\xi_1 x_1 r_2^2}{R^4} - \ln R \right\}$$

$$\overline{C}_{1212} = K_e \left\{ -\frac{r_1 r_2}{r^2} - (1-\nu)\alpha_1 + \frac{(x_1-\xi_1)r_2}{R^2} - \frac{4\xi_1 x_1 R_1 r_2}{R^4} + 2\nu(1-\nu)\alpha_2 \right\}$$

$$\overline{C}_{1222} = K_e \left\{ \frac{r_1^2}{r^2} + \ln r + \frac{3x_1^2 - \xi_1^2 + 4\xi_1 x_1}{R^2} - \frac{4\xi_1 x_1 R_1^2}{R^4} - \ln R \right\}$$

$$\overline{C}_{2211} = K_e \left\{ -\frac{r_1 r_2}{r^2} + 2\nu\theta_1 + \frac{[x_1 - (1-4\nu)\xi_1]r_2}{R^2} + \frac{4\xi_1 x_1 R_1 r_2}{R^4} - 2\nu\theta_2 + 4(1-\nu)^2\alpha_2 \right\}$$

$$\overline{C}_{2212} = K_e \left\{ -\frac{r_1^2}{r^2} + (1-2\nu)\ln r + \frac{-x_1^2 - (1-4\nu)\xi_1^2 - 4(1-\nu)\xi_1 x_1}{R^2} + \frac{4\xi_1 x_1 R_1^2}{R^4} - (1-2\nu)\ln R \right\}$$

$$\overline{C}_{2222} = K_e \left\{ -\frac{r_1 r_2}{r^2} + 2(1-\nu)\theta_1 + \frac{[3x_1 + (1-4\nu)\xi_1]r_2}{R^2} - \frac{4\xi_1 x_1 R_1 r_2}{R^4} + 2(1-3\nu)\theta_2 + 4(1-\nu)\alpha_2 \right\}$$

with:

$$K_e = \frac{E}{4\pi(1-\nu^2)}$$